Downloaded 11/05/14 to 142.51.108.254. Redistribution subject to SEG license or copyright; see Terms of Use at http://library.seg.org/

Conductance estimates from spatial and temporal derivatives of borehole electromagnetic data

Michal Kolaj and Richard Smith, Laurentian University*

Summary

The conductance of an infinite uniformly conductive thin sheet can be calculated using the ratio of the temporal gradient and the gradient in the normal direction of any component (or combination of components) of the secondary magnetic field. With standard borehole electromagnetic (BHEM) systems, both gradients can be readily calculated using finite difference approximations. For a finite thin sheet, synthetic modeling demonstrated that the magnitude of the field provided a robust and reliable apparent conductance in typical 3-component BHEM survey configurations. In a field example of BHEM data collected over a massive sulfide deposit in Sudbury, Ontario, Canada, the spatial gradient could be calculated over a roughly 100 m wide zone and a consistent apparent conductance could be calculated at each delay time using the magnitude of the field. Increases in the apparent conductance estimate with increasing delay time are likely due to currents migrating into more conductive parts of the body. The apparent conductance values are also consistent with Maxwell models. This simple and robust apparent conductance is ideal as a first pass estimate for target discrimination, grade estimation and starting values for modeling and inversion.

Introduction

The success of inductive borehole electromagnetic (BHEM) methods in the exploration for base metals can be attributed to the methods' ability to detect conductive mineralization (which is often the deposit itself) and other conductive geological features of interest (Dyck, 1991). In massive sulfide exploration, the contrast in conductivity between crystalline basement rock and massive sulfides can be as high as 10^9 and with exploration in mature districts such as Sudbury, Ontario, Canada often exceeding depths of 1 km, BHEM is often the primary tool for geophysical exploration and characterization (King, 2007).

The quantitative forward and inversion modeling approach in mineral exploration BHEM varies from manual methods (the interpreter generates synthetic models, using software such as "MultiLoop", until the synthetic data resembles the field data, Lamontagne, 2007); to semi-automated methods (the interpreter generates a model which somewhat resembles the field data and then automated inversion fine-tunes the model to provide a better match) to the less common but nearly fully automated methods (inversion algorithms such as the one found in Zhang and Xiao, 2001). In mineral exploration, the targets (especially massive sulfides) can often be well represented as thin sheets and many BHEM interpretation procedures take advantage of this (Grant and West, 1965; Palacky 1987; Polzer 2000; King 2007). Like the majority of quantitative geophysical techniques, many of these routines are complicated, suffer from non-uniqueness and the output model may depend strongly on having reliable starting information (Li and Oldenburg, 2000; Oldenburg and Pratt, 2007; Lamontagne 2007; Lelievre et al., 2009). It is convenient to have a simple method to calculate the conductance directly from BHEM data.

Three benefits of having reliable estimates of conductivity or conductance (product of conductivity and thickness) are 1) to have better starting models for modeling and inversions; 2) for improved target discrimination (King, 2007); and 3) an ability to estimate grade variation within the target (McDowell et al., 2007).

The method presented in this paper uses the formulation of Kolaj and Smith (2013), whom developed a methodology to estimate the conductance of a thin sheet from time-domain EM data using the ratio of the temporal gradient and the gradient in the vertical direction of the vertical secondary magnetic field. We show that for an infinite uniform sheet, any magnetic field component (or combination of components) can be used to estimate the conductance. Through synthetic studies and field data collected in Sudbury, Ontario, Canada, we show that the magnitude of the magnetic field can be used to calculate a reliable and robust apparent conductance over finite sized sheets using typical 3-component BHEM surveys.

Method

Following Price (1949), Smith and West (1987), and Kolaj and Smith (2013), the relationship between magnetic fields for a flat-lying uniform conductance thin sheet in a resistive medium is,

$$C = \frac{2}{\mu}\left(\frac{\frac{dH_n^s}{dn}}{\frac{dH_n}{dt}}\right), \qquad (1)$$

where C is the conductance of the sheet, μ is the magnetic permeability (generally assumed to be that of free space), dH_n^s/dn, and dH_n/dt are spatial and temporal derivatives (in the direction of the normal, n, to the sheet direction), $\mathbf{H}^S$ represents the secondary field emanating from the sheet and $\mathbf{H}$ represents the total field (secondary field plus the

© 2014 SEG

DOI http://dx.doi.org/10.1190/segam2014-0132.1

Downloaded 11/05/14 to 142.51.108.254. Redistribution subject to SEG license or copyright; see Terms of Use at http://library.seg.org/

primary field from the transmitter, $\mathbf{H} = \mathbf{H}^S + \mathbf{H}^P$). In the off-time or when the primary field is constant, the temporal derivative will be solely a secondary field (i.e. $dH_n^P/dt = 0$). This ratio can therefore be independent of the transmitter (location and current waveform) which adds to the simplicity of the method. If the sheet does not have a uniform conductance or is finite, then equation 1 will not yield a conductance, but an apparent conductance. Equation 1 requires measurements of both the magnetic field and its time derivative, which can be obtained by using a magnetic field sensor and then estimating its time derivative using adjacent delay times or, alternatively, if using an induction coil (time derivative) sensor, then the full-waveform time derivative measurements can be integrated to give a magnetic field (Smith and Annan, 2000). The derivative in the normal direction of the magnetic field can then be approximated using the difference between adjacent stations.

Equation 1 can be investigated in more detail using image theory in cylindrical coordinates (Grant and West, 1965). If the transmitting source is a vertical dipole situated at (0, h) with moment m and the infinite sheet of conductance, C, is located in the plane $z = 0$ then the derivatives can be shown to be equal to

$$\frac{d\mathbf{H}^S}{dz}(\rho,z,t) = \frac{3m}{4\pi}\left[\frac{\rho(\rho^2-4a^2)}{(\rho^2+a^2)^{\frac{7}{2}}}\mathbf{i}_p + \frac{a(3\rho^2-2a^2)}{(\rho+a^2)^{\frac{7}{2}}}\mathbf{i}_z\right] \qquad (2)$$

and

$$\frac{d\mathbf{H}^S}{dt}(\rho,z,t) = \frac{3m}{2\pi\mu C}\left[\frac{\rho(\rho^2-4a^2)}{(\rho^2+a^2)^{\frac{7}{2}}}\mathbf{i}_p + \frac{a(3\rho^2-2a^2)}{(\rho^2+a^2)^{\frac{7}{2}}}\mathbf{i}_z\right], \qquad (3)$$

where $a = z + h + (2t/\mu C)$ and $\mathbf{i}_\rho$ and $\mathbf{i}_z$ are the unit vectors along the ρ and z axes, respectively (there is no field in the φ direction as the primary field has no component in this direction, Telford et al., 1990). This is known as Maxwell's receding image solution (Grant and West, 1965) as the secondary magnetic fields are equal to the image of the source receding away at a velocity of $(2/\mu C)$. Notice that the terms on the right-hand-side in square brackets are identical. Thus, by dividing the vertical components of equation 2 and 3, a factor of $(\mu C/2)$ remains which is the expected result based upon equation 1. However, as evident in equations 2 and 3, this relationship is also true for other components of the vector, specifically H_ρ. As all the components result in the same answer, any linear combination of the components, including the magnitude, $H_m = (H_\rho^2 + H_z^2)^{0.5}$, can be used in the calculation of the conductance.

While any component can be used to calculate the conductance of an infinite uniformly conductive sheet, it is not as easy to prove how effective the different components will be at calculating an apparent conductance of finite non-uniform thin sheets. This will be further investigated through forward modeling of finite thin sheets in the following section.

Synthetic Example

A 1 Hz BHEM UTEM survey (West et al., 1984) with station spacing of 10 m was simulated in MultiLoop III (Lamontagne Geophysics). A general schematic of the synthetic model can be seen in Figure 1. Since a UTEM survey measures the magnetic field at each station, the spatial derivative was calculated using a central difference between adjacent stations and the time derivative was calculated using adjacent delay times. Since the time derivative is calculated using adjacent delay times, the spatial derivative is also averaged over the same adjacent delay times. Note that no noise (apart from some numerical noise) was added to the data.

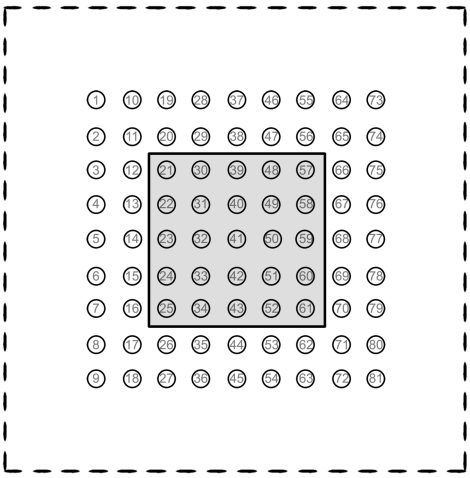

Figure 1. Plan view of the generalized survey geometry for the synthetic models used in MultiLoop III. Dashed black line represents the transmitter loop, circles represent the boreholes (numbered 1-81, spaced 50 m apart) and the central grey square represents the thin sheet.

In the first example, a 600 m by 600 m loop was positioned around the survey area (Figure 1) containing a 250 m by 250 m sheet at a depth of 200 m having a conductance of 10,000 S with boreholes (BH) oriented normal to the sheet (i.e. no dip). A gridded map of the apparent conductance from all boreholes at channel 2 (late time) at a depth of 180 m (20 m above the sheet) can be seen in Figure 2. Earlier time data produced similar results but with slightly smaller calculated conductance values. For the vertical component (H_z), there seemed to be an edge effect for stations in close proximity to the sheet edge at a depth of 180 m, so for these holes, the estimate from a depth of 190 m was used. Similarly, for the horizontal component (H_ρ) there were erroneously high apparent conductance values for the boreholes that did not intersect the sheet and a depth of 160

© 2014 SEG

DOI http://dx.doi.org/10.1190/segam2014-0132.1

Downloaded 11/05/14 to 142.51.108.254. Redistribution subject to SEG license or copyright; see Terms of Use at http://library.seg.org/

m for these holes resulted in improved results. These issues were not seen in the estimates obtained using the magnitude (H_m), suggesting this may be a more robust method. In Figure 2, H_z produces a relatively diffuse anomaly and the apparent conductance drops off steadily away from the sheet center. The image from H_ρ is less diffuse but the apparent conductance over-estimates the actual conductance over the majority of the sheet and contains some edge effects for the non-intersecting boreholes. The H_m image has all of the sought characteristics: high resolution, minimal boundary effects and a consistent apparent conductance estimate over the majority of the sheet. While each method would likely provide an apparent conductance of about the same order of magnitude, H_m appears to be superior.

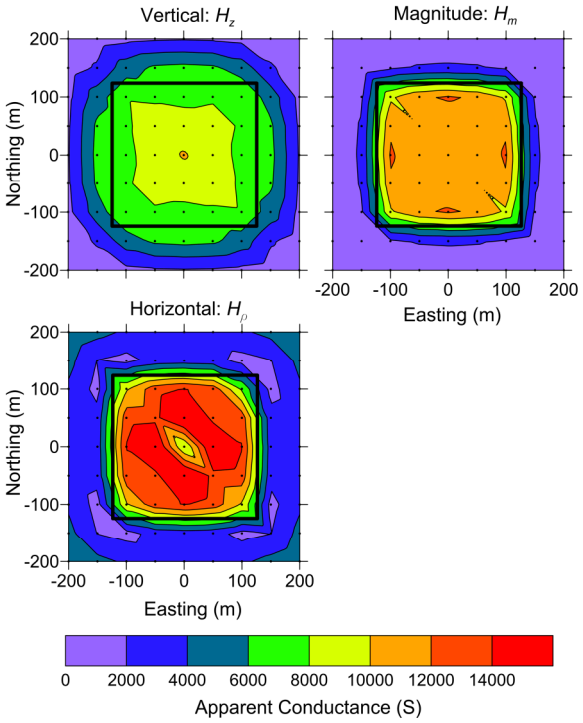

Figure 2. Gridded apparent conductance at late time (t = 140.6 ms) using H_z (top left), H_m (top right) and H_ρ (bottom left) corresponding to the survey layout seen in Figure 1. Black dots represent borehole locations and the thick black line is the outline of the 10,000 S sheet. The image is generated from estimates at a depth of approximately 180 m (see text).

The effects of having a non-zero sheet dip and varying transmitter loop locations were also investigated. In all studied situations, it was found that when the conductance is calculated using H_m there is a well-defined sheet edge, minimal edge effects and a relatively consistent apparent conductance over the sheet. With a non-zero dip the spatial gradient is no longer calculated along the normal direction but rather along the borehole axes. This tended to produce smaller apparent conductance values but the approximation was found to be adequate as long as the distance between stations is small and the secondary magnetic fields are not rapidly varying over that small distance.

It should also be mentioned that with real survey data it would likely not be possible to calculate the apparent conductance down the entire hole due to low signal levels in the spatial gradient ($d\mathbf{H}/dz$). In reality, an adequate signal-to-noise ratio and thus calculated apparent conductance may only be possible where the fields are large (as would be the case in close proximity to the target). Therefore, using the magnitude component has the added benefit that the magnitude of the field will be the largest possible combination of the components and will thus produce the best possible signal-to-noise ratio.

Field example

The presented methodology for estimating a down-hole conductance can be readily applied to existing borehole data since the method requires 3-component data which is generally the standard in modern BHEM. As such, a previously surveyed borehole (4 Hz UTEM survey with a station spacing ranging from 10 m to 15 m) in Sudbury, Ontario, Canada was used in this study. The massive sulfide deposits in Sudbury were chosen as ideal targets as they can generally be well approximated by one or more thin sheets/plates which is a situation consistent with the assumptions of the method. The results of equation 1 using H_m can be seen in Figure 3.

The magnitude of the field (Figure 3A) was calculated from the 3-component data and it is clear that, apart from a roughly 100 m wide zone, the fields are very small over the majority of the hole. The spatial gradient was calculated using the distance down-hole (z_m) rather than the change in elevation. The borehole is essentially vertical and as such, the difference is negligible. The derivatives (dB_m/dt and dB_m/dz_m, Figure 3B-C respectively) were calculated using the same finite difference scheme as in the synthetic study. Since spatial gradients have very low signal values, dB_m/dz_m is erratic over the majority of the hole due to the low signal-to-noise ratio. As such, the apparent conductance could only be calculated over a small section of the hole where the fields were large (Figure 3D, where dB_m/dz_m is above a few pT). This is not much of an issue as the fields are expected to be the largest in the areas of closest proximity to the target and that is also where the apparent conductance (equation 1) is the most reliable.

Most apparent conductance values fall between 1000 S to 10,000 S and while the apparent conductance values do span a large range, the apparent conductance is relatively constant over the depth range at each delay time. The field values show large variations from 300 to 400 m depth across the peak in Figure 3A-C but the apparent conductance values for each delay time are more or less similar across the same depth range. Since the results are

© 2014 SEG

DOI http://dx.doi.org/10.1190/segam2014-0132.1

Downloaded 11/05/14 to 142.51.108.254. Redistribution subject to SEG license or copyright; see Terms of Use at http://library.seg.org/

consistent, this supports the hypothesis that the apparent conductance estimates are reliable. The increase in apparent conductance with delay time was also seen in synthetic examples but the range is larger in the field example. It is possible that this discrepancy is due to the inapplicability of the thin-sheet assumption. Furthermore, with highly conductive bodies, the early time data represents currents which are mainly confined to the surface of the conductor and are only weakly dependent on the conductivity structure in the core of the body (Grant and West, 1965). With increasing delay time, the established currents diffuse into the body and the behavior of the magnetic field will reflect the more conductive parts of the body. This is likely the reason why there is a large change in the apparent conductance from early to late time.

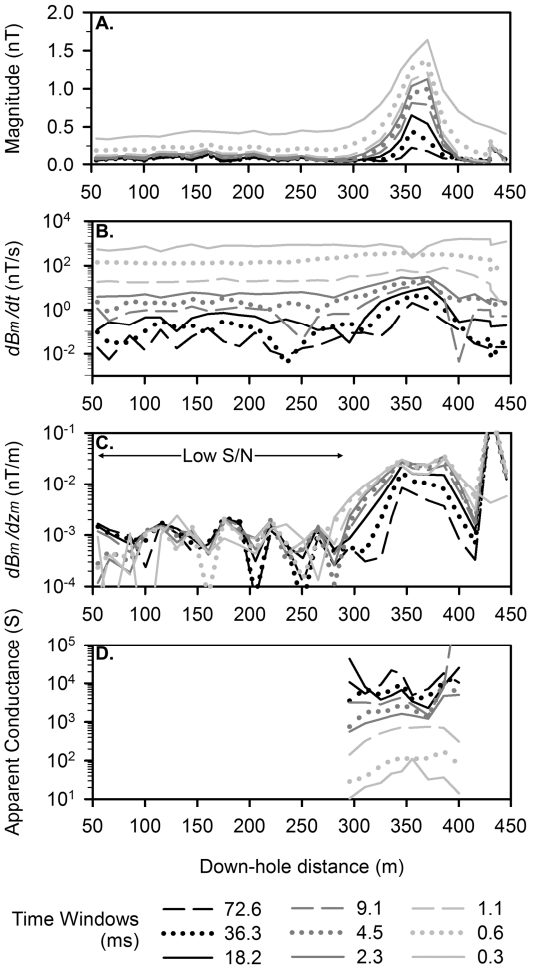

Figure 3. Results from a 4 Hz borehole UTEM survey A. Magnitude of the magnetic field (B_m). B. Absolute magnitude of the temporal derivative (dB_m/dt). C. Absolute magnitude of the spatial gradient (dB_m/dz_m), area of low signal-to-noise (S/N) ratio indicated. D. Apparent conductance as calculated using equation 1 over the acceptable S/N ratio region.

The mean log apparent conductance over 310 m to 390 m for channels 2 to 4 (36.3 ms to 9.1 ms, respectively) ranges from roughly 3400 S to 6400 S. The data was also modeled in Maxwell (software by ElectroMagnetic Imaging Technology Pty Ltd) using conductance values of 3000 S, respectively (S. Dickie, personal communication, 2013) which is consistent with our results. If there were multiple drill holes intersecting the target, then it would be possible to image the apparent conductance variation over the targets in a similar way to the synthetic example.

Conclusion

The conductance of an infinite uniform thin sheet can be calculated from any magnetic field component (or combination of components) by taking the ratio of the spatial derivative in the normal direction with the temporal derivative. Through synthetic modeling we show that by using the magnitude of the magnetic field, reliable apparent conductances of finite sized sheets can also be obtained. This methodology is ideal for BHEM data, where a geophysicist typically estimates the conductance though a laborious process of forward modeling the data. In real field data, a limiting factor is the accuracy in which the spatial gradient can be calculated with a finite difference approach between adjacent stations as spatial gradient signals are quite low. However, we show from BHEM data acquired in a massive sulfide example in Sudbury, Ontario, Canada that the spatial gradient is large enough in proximity to the sheet (up to 100 m in this example) and an apparent conductance estimate could be obtained. The estimated value is smaller at early delay times but as large as 10,000 S at later delay times. The apparent conductance values are also consistent with Maxwell models. Estimating the target's conductance from a simple ratio derived from BHEM data is an attractive complement to i) logging the hole with a conductivity probe, ii) traditional inversions and forward modeling and iii) using handheld instruments or laboratory techniques on the recovered core.

Acknowledgments

We are grateful to the following for financial support of this research: NSERC, Vale, Sudbury Integrated Nickel Operations, a Glencore Company, Wallbridge Mining, KGHM International and the Centre for Excellence in Mining Innovation. In particular, we would like to also thank Sean Dickie and Ben Polzer whose feedback and assistance improved the work. M. Kolaj is grateful for the NSERC Alexander Graham Bell, the George V. Keller and the SEG/KEGS Ontario scholarships. Multiloop III was provided by Lamontagne Geophysics and Peter Walker guided us in its use.

© 2014 SEG

DOI http://dx.doi.org/10.1190/segam2014-0132.1

http://dx.doi.org/10.1190/segam2014-0132.1

EDITED REFERENCES

Note: This reference list is a copy-edited version of the reference list submitted by the author. Reference lists for the 2014 SEG Technical Program Expanded Abstracts have been copy edited so that references provided with the online metadata for each paper will achieve a high degree of linking to cited sources that appear on the Web.

REFERENCES

Dyck, A. V., 1991, Drill-hole electromagnetic methods, *in* M. N. Nabighian, ed., Electromagnetic methods in applied geophysics, vol. 2: SEG, 881–930.

Grant, F. S., and G. F. West, 1965, Interpretation theory in applied geophysics: McGraw-Hill Book Company.

King, A., 2007, Review of geophysical technology for Ni-Cu-PGE deposits: Proceedings of the 5th Decennial International Conference on Mineral Exploration, 647–665, www.dmec.ca/ex07-dvd/E07/pdfs/45.pdf.

Kolaj, M., and R. S. Smith, 2013, Using spatial derivatives of electromagnetic data to map lateral conductance variations in thin sheet models: Applications over mine tailings ponds: Geophysics, **78**, no. 5, E225–E235, http://dx.doi.org/10.1190/geo2012-0457.1.

Lamontagne, Y., 2007, Deep exploration with EM in boreholes: Proceedings of the 5th Decennial International Conference on Mineral Exploration, 401–415.

Lelièvre, P. G., D. W. Oldenburg, and N. C. Williams, 2009, Integrating geological and geophysical data through advanced constrained inversions: Exploration Geophysics, **40**, no. 4, 334–341, http://dx.doi.org/10.1071/EG09012.

Li, Y., and D. W. Oldenburg, 2000, Incorporating geological dip information into geophysical inversions: Geophysics, **65**, 148–157, http://dx.doi.org/10.1190/1.1444705.

McDowell, G., A. Mackie, and M. Palkovits, 2007, Grade estimation at CVRD Inco's Canadian sulphide mines: Proceedings of the Symposium on the Application of Geophysics to Engineering and Environmental Problems (SAGEEP), Environmental & Engineering Geophysical Society, 1103–1112.

Oldenburg, D. W., and D. A. Pratt, 2007, Deep exploration with EM in boreholes: Proceedings of the 5th Decennial International Conference on Mineral Exploration, 61–95.

Palacky, G. J., 1987, Resistivity characteristics of geological targets, *in* M. N. Nabighian, ed., Electromagnetic methods in applied geophysics, vol. 1: SEG, 53–125.

Polzer, B., 2000, The role of borehole EM in the discovery and definition of the Kelly Lake Ni-Cu deposit, Sudbury, Canada: 70th Annual International Meeting, SEG, Expanded Abstracts, 1063–1066.

Price, A. T., 1949, The induction of electric currents in non-uniform thin sheets and shells: The Quarterly Journal of Mechanics and Applied Mathematics, **2**, no. 3, 283–310, http://dx.doi.org/10.1093/qjmam/2.3.283.

Smith, R. S., and A. P. Annan, 2000, Using an induction coil sensor to indirectly measure the B-field response in the bandwidth of the transient electromagnetic method: Geophysics, **65**, 1489–1494, http://dx.doi.org/10.1190/1.1444837.

Downloaded 11/05/14 to 142.51.108.254. Redistribution subject to SEG license or copyright; see Terms of Use at http://library.seg.org/

Smith, R. S., and G. F. West, 1987, Electromagnetic induction in an inhomogeneous conductive thin sheet: Geophysics, **52**, 1677–1688, http://dx.doi.org/10.1190/1.1442284.

Telford, W. M., L. P. Geldart, and R. E. Sheriff, 1990, Applied geophysics: Cambridge University Press.

West, G. F., J. C. Macnae, and Y. Lamontagne, 1984, A time-domain EM system measuring the step response of the ground: Geophysics, **49**, 1010–1026, http://dx.doi.org/10.1190/1.1441716.

Zhang, Z., and J. Xiao, 2001, Inversions of surface and borehole data from large-loop transient electromagnetic system over a 1-D earth: Geophysics, **66**, 1090–1096, http://dx.doi.org/10.1190/1.1487056.

Downloaded 11/05/14 to 142.51.108.254. Redistribution subject to SEG license or copyright; see Terms of Use at http://library.seg.org/